IEEE Access
Multidisciplinary | Rapid Review | Open Access Journal

Received October 15, 2020, accepted October 24, 2020, date of publication October 28, 2020, date of current version November 12, 2020.

Digital Object Identifier 10.1109/ACCESS.2020.3034314

MF-HER: Marine Mammal-Friendly Based High Spectral-Efficient Routing for Underwater Acoustic Sensor Networks

YOUGAN CHEN[1,2,3], (Senior Member, IEEE), XINRUI ZHANG[1,2,3], XIANG SUN[4], (Member, IEEE), YI TAO[1,2,3], (Member, IEEE), AND XIAOMEI XU[1,2,3]

[1]Key Laboratory of Underwater Acoustic Communication and Marine Information Technology (Xiamen University), Ministry of Education, Xiamen 361005, China
[2]College of Ocean and Earth Sciences, Xiamen University, Xiamen 361102, China
[3]Shenzhen Research Institute of Xiamen University, Shenzhen 518000, China
[4]Department of Electrical and Computer Engineering, University of New Mexico, Albuquerque, NM 87131, USA

Corresponding author: Yougan Chen (chenyougan@xmu.edu.cn)

This work was supported in part by the Basic Research Program of Science and Technology of Shenzhen, China under Grant JCYJ20190809161805508; in part by the Xiamen University Undergraduate Innovation and Entrepreneurship Training Programs under Grant 201810384097; in part by the Fundamental Research Funds for the Central Universities of China under Grant 20720180078; and in part by the National Natural Science Foundation of China under Grant 41476026, Grant 41676024, and Grant 41976178.

ABSTRACT In real ocean environments, artificial acoustic and natural acoustic systems are coexisted to share scarce spectrum resources. In this paper, we propose a marine mammals-friendly based high spectral-efficient routing (MF-HER) protocol to improve spectrum utilization and protect marine mammal communications in underwater acoustic sensor networks (UW-ASNs), which makes full use of the interlacing frequency bands that are shared by both marine mammals and UW-ASNs. In the proposed MF-HER protocol, the detour strategy is adopted to adaptively avoid the interference of acoustic radiation from sensor nodes to the acoustic communication habits of marine mammals. Meanwhile, the non-detour strategy is adopted if there is no marine mammal or the marine mammals do not use the same frequency bands for communication in the sea area, and thus the sensor nodes can fully utilize the frequency bands without interference from the marine mammals. Due to the diversity of acoustic frequency bands used by marine mammals, the reasonable design of a routing protocol can shorten the distance of forwarding path and optimize the performance of UW-ASNs while protecting marine mammals. Simulation results show that, as compared to the existing bio-friendly routing protocol of UW-ASNs, the proposed MF-HER protocol can effectively improve the energy consumption of the sensor nodes, bit error rate, and network throughput, while avoiding the communication masking effect among marine mammals.

INDEX TERMS Marine mammals, high spectral-efficient, underwater acoustic networks, energy consumption, bit error rate, network throughput.

I. INTRODUCTION

Ocean, covering more than 70% of the earth's surface, contains enormous amount of resources and energy. The complexity of underwater environment brings severe challenges to achieve underwater data transmissions. Different from terrestrial wireless sensor networks, electromagnetic radio waves decay severely when they propagate in the water. The most effective way for underwater data transmissions and networking is to use acoustic waves as the carrier. Underwater acoustic sensor networks (UW-ASNs), which show the great potential to benefit underwater communications, have received increasing attention recently and become a new research hotspot. UW-ASNs have been applied to many underwater applications, such as earthquake monitoring, oilfield exploitation [1], pollution and environmental monitoring, offshore exploration [2], disaster prevention, and assisted navigation [3].

The associate editor coordinating the review of this manuscript and approving it for publication was Jiajia Jiang.

In the past few decades, terrestrial wireless sensor networks have been developed and explored rapidly. The routing protocols for the terrestrial wireless networks can be generally classified into three categories, i.e., the proactive routing, passive routing, and geographical routing protocols [4]. Although many high performance routing protocols have been designed for terrestrial wireless networks, they cannot work properly in UW-ASNs due to the complex underwater conditions, such as the dynamics of water temperature and pressure, Doppler effect, and underwater noise caused by ocean currents, marine biological activities, etc.

More specifically, the propagation speed of acoustic signals in water is approximately 1.5×10^3 m/s, which is five times of magnitude lower than that of radio waves in air (3×10^8 m/s) [5], resulting in a longer end-to-end delay in UW-ASNs. In addition, the data transmissions in UW-ASNs experience serious losses of signals [6], complex multi-path effect [7], and severe Doppler effect, which lead to high bit error rate [1] and energy consumption. Meanwhile, since a higher carrier frequency results in higher transmission loss and absorption loss of acoustic waves underwater, the low-frequency transmission technology is usually adopted for underwater acoustic data transmissions. Hence, the available bandwidth of underwater acoustic communications is very limited, and so the data rate is very low. In underwater environments, artificial acoustic and natural acoustic systems are coexisted, i.e., they have to share the scarce spectrum resources. The existence of marine mammals in the natural acoustic system makes the design of efficient UW-ASNs much more challenging and demanding. Undoubtedly, UW-ASNs could affect the original life of marine mammals to some extent. All the mentioned uniqueness of underwater environment requires designing a novel routing protocol tailored for UW-ASNs.

Many researchers have proposed various routing protocols to solve different issues in UW-ASNs. As a basic geographic routing protocol, vector based forwarding (VBF) is proposed in the context of mobile UW-ASNs [8]. Each packet is assumed to contain the information of the locations of the source, destination, and forward nodes. These information are used to predetermine a ''virtual routing pipe'' between each source and destination nodes, and only the sensor nodes in the virtual routing pipe can forward the related data packets. However, these virtual routing pipes are determined based on the layout of sensor nodes, and may cause routing holes. Hop-to-hop vector based forwarding (HH-VBF) is proposed [9] to solve the routing hole problem. Instead of establishing a virtual routing pipe from a source to a destination node, HH-VBF creates a virtual routing pipe for each wireless hop. Although HH-VBF solves the routing hole problem, it incurs higher end-to-end delay and energy consumption. The new vector based forwarding (N-VBF) [10] and lifetime-extended vector-based forwarding (LE-VBF) protocols [11] are proposed. As compared to HH-VBF, N-VBF has lower energy efficiency but lower network latency and LE-VBF incurs higher energy efficiency but higher network latency. Other routing protocols, whose design concepts are deviated from VBF, are explored. The depth-based routing (DBR) protocol is proposed to route packets based on the depth of sensor nodes in the network [29]. DBR tries to optimize the routing algorithm in the depth direction such that the lifetime of the network can be prolonged. However, DBR is designed based on broadcast medium access control (MAC), which could bring severe packet collisions for sensed data transmissions in UW-ASNs. The DBR aware MAC protocol, entitled DBR-MAC, is proposed [23]. DBR-MAC adopts a cross-layer approach to smoothly integrate a handshaking-based MAC mechanism with DBR to mitigate the packet collision problem. In addition, a novel machine-learning-based adaptive routing protocol is proposed [3], which tries to a shortest forwarding path for each source-destination pair in order to improve the energy efficiency of data transmission, and extend the lifetime of the network. Yet, the convergence speed of the proposed machine-learning-based adaptive routing protocol is slow, and so is not suitable for large-scale UW-ASNs.

All the mentioned routing algorithm, however, do not take the communication masking effect in marine mammals [31], [32] (where UW-ASNs may interfere with the acoustic signals used by marine mammals for communication, positioning and navigation) into consideration. Due to the scarcity of underwater spectrum resources, UW-ASNs and marine mammals have to share the same frequency band in the time division multiplexing manner to mitigate the interference and maintain the daily lives of marine mammals. Therefore, it is necessary to design a routing protocol for UW-ASNs to minimize the interference. Few literatures have explored the solutions on this challenge. By estimating locations of marine mammals, Yao *et al.* [12] constructed an environment-friendly spectrum decision strategy, which jointly optimizes the transmission power and wireless channel allocation to the contending sensors in order to avoid the interference to the marine mammals while maximizing the network capacity. The proposed strategy, however, is unable to allocate wireless channels to a sensor node pair when marine mammals are located in the line-of-sight area between the sensor node pair. Jin *et al.* [13] presented the bio-friendly cognitive underwater routing (BF-CAR) protocol, which adopts the detour routing in the network layer to address the above issue. The BF-CAR protocol not only avoids the interference to the communication of marine mammals but also ameliorates the network performances as compared to traditional routing protocols. However, BF-CAR does not consider if acoustic signals of marine mammals could be affected by the communications in UW-ASNs, but simply carries out detour forwarding paths away from the nearby marine mammals, thus unable to fully utilize the underwater acoustic spectrum resources. Specifically, the acoustic signals of marine mammals are classified into three categories, i.e., whistles, clicks, and burst pulse [14]. These three types of signals correspond to different frequency ranges. Only the frequency range occupied by whistles overlaps with the

frequency range of UW-ASNs. Hence, it is not necessary to choose detour forwarding paths in UW-ASNs if the frequency range of whistles is unused. This is the original intention of this work.

In this paper, we propose a novel routing protocol, i.e., marine mammals-friendly based high spectral-efficient routing (MF-HER), which improves the BF-CAR protocol to get better network performances.

The main contributions of this paper are as follows:

1) In the proposed MF-HER protocol, the bioacoustic properties of marine mammals have been introduced and integrated into the design and analysis of the routing protocol in UW-ASNs. The behavioral response threshold and auditory sensitivity threshold of marine mammals are analyzed, and then the maximum sound pressure level acceptable to marine mammals is derived. According to the sound pressure level of marine mammals as well as the relationship between the transmission loss of underwater acoustic signals and the transmission distance, the acoustic protection based safety distance between the sensor nodes and marine mammals can then be determined.

2) The proposed MF-HER protocol applies the adaptive detour strategy based on acoustic communication habits of marine mammals. That is, the detour strategy is applied only if the frequency range of UW-ASNs is used by marine mammals; otherwise, the non-detour strategy is applied. This can significantly improve underwater acoustic spectrum resource utilization.

3) The performance of the MF-HER protocol (in terms of energy consumption, bit error rate, and network throughput) is compared to the BF-CAR protocol via extensive simulations.

The rest of this paper is organized as follows. In Section II, we present the system models and the proposed MF-HER protocol. In Section III, the performance of the proposed protocol is theoretically evaluated. The simulation results and analysis are presented in Section IV. Conclusions are given in Section V.

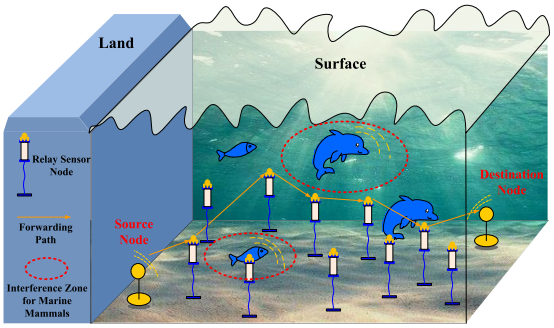

FIGURE 1. The schematic diagram of UW-ASNs system including marine mammals.

II. SYSTEM MODEL AND THE PROPOSED MF-HER PROTOCOL

A. THE MARINE MAMMAL-FRIENDLY UW-ASNS SYSTEM

In a UW-ASN shown in Fig. 1, when acoustic signals are forwarded from a source to a destination node, they most likely pass the area near the marine mammals, thus interfering with marine mammals' communication. Here, we define the interference zone of a marine mammal as the area where all the sensor nodes may interference to the marine mammal's communication. Specifically, as shown in Fig. 2, denote R_{m} as the maximum radius that the hearing threshold of a marine mammal can reach. Denote R_{n} as the maximum propagation radius of a sensor node. Then, the interference zone of the marine mammal is a circle (i.e., dotted red line in Fig. 2) with the center equal to the marine mammal's position and the radius R_{s} equal to $R_{\mathrm{m}} + R_{\mathrm{n}}$. Note that the position of marine mammals and R_{m} can be perceived by applying the underwater acoustic cognition technology, as described in [13].

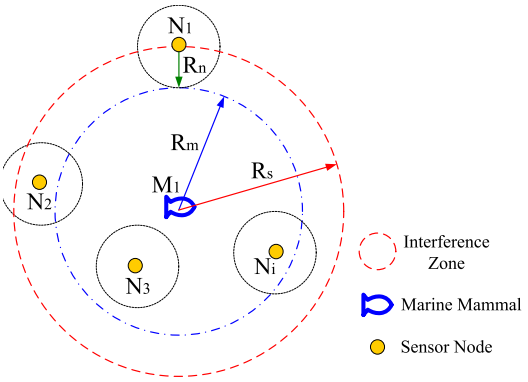

FIGURE 2. The interference zone for marine mammals in UW-ASNs.

If there is an interference zone overlapping with the forwarding path from the transmitting node to the receiver node for a wireless hop, then a detour forwarding path will be calculated and adopted. For example, Fig. 3(a) shows a 2-hop non-detour forwarding path with source node S, destination node D, and several possible relay nodes N_i ($i = 1, 2, \ldots$), which are located within the maximum propagation radius of source node S. The relay node, which has the smallest angle $\angle\alpha_{\mathrm{i}}$ ($i = 1, 2, \ldots$) among other possible relay nodes, will be selected to relay the packets. Fig. 3(b) shows an example of the detour forwarding path. When data packets are forwarded from source node S to destination node D via relay node N_1, the relay node N_1 may detect the interference from a marine mammal as N_1-D forwarding path is overlapped with the interference zone of the marine mammal. Thus, a detour forwarding path is calculated by relay node N_1. In this example, S-N_1-N_2-D instead of S-N_1-N_3-D is selected as the detour path to mitigate the interference since the length of line V-N_2 is shorter than that of line V-N_3, where V is the perpendicular intersection of lines N_1-D and N_2-N_3. Note that once source node S realizes the detour forwarding path to destination node D, a new path S-N_2-D shown in Fig. 3(c) will be applied to bypass the interference zone. Fig. 3(d) shows the case that many interference zones are existed and how the detour forwarding path is derived.

Note that, when a marine mammal is located in the line-of-sight of the source and destination nodes, the interference to the marine mammal is the strongest. For example, if the

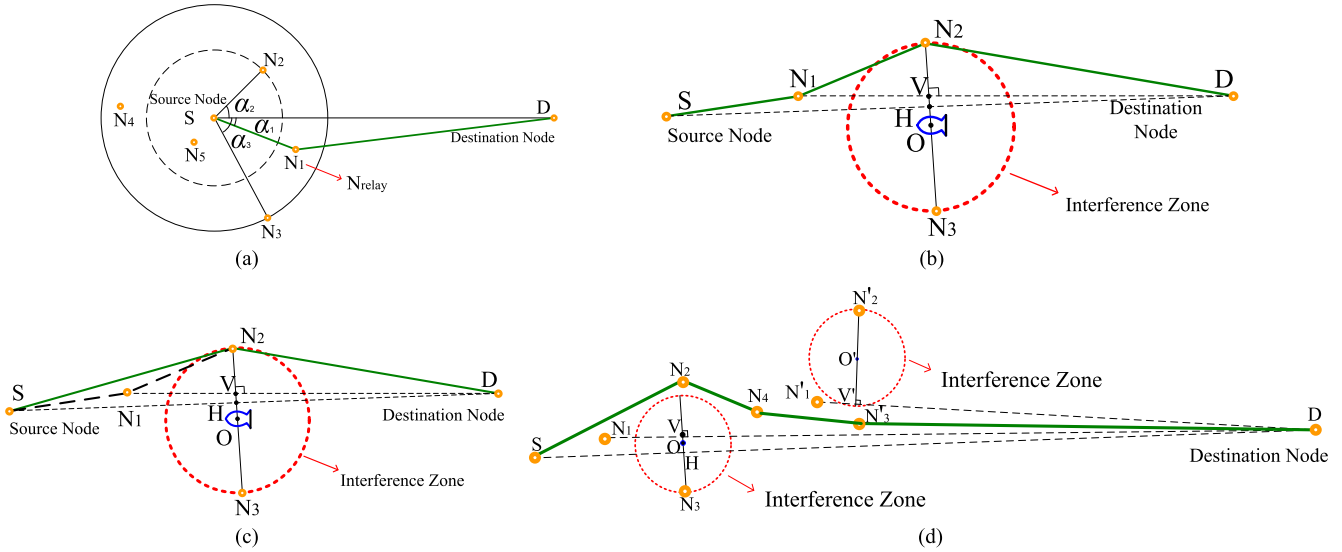

FIGURE 3. The diagram of illustrating detour schemes: (a) the 2-hop non-detour forwarding path; (b) the detour forwarding path; (c) the detour forwarding path change; (d) a complete multi-hop packets transmission process for a multiple interference zones case.

location of the marine mammal, denoted as O, is in the line S-D in Figs. 3(b), 3(c), and 3(d), the interference to the marine mammal is the strongest.

B. EFFECTS OF UNDERWATER ACOUSTIC COMMUNICATION ON MARINE MAMMALS

The exploitation and utilization of the ocean have seriously affected the normal life of marine mammals. Environmental pollution has destroyed their living environment. Over the last six decades, background noise levels have been doubled every decade, mainly because of shipping, with an increase of 20 dB in 50 years in some areas, which has a devastating impact on underwater lives [15]. In order to accurately understand how the man-made strong noise sources impact on marine lives, people began to monitor and study marine environment noise in 1990s. For example, in 1997, the U.S. Geological Survey (USGS) proposed 180 dB re $1\mu Pa^2s$ is the sound exposure level (SEL) threshold of potential harm to marine mammals in terms of behavior, physiology, and hearing effects through field exploration [15]. Subsequently, many countries promulgated relevant laws to limit intensity of man-made underwater noises to protect underwater lives.

Man made marine environment noises include ship noise, industrial noise, etc. UW-ASNs have recently been concerned to have a significant influence on marine mammals as well. The underwater acoustic communications among sensor nodes in the UW-ASNs is also a type of artificial noise that can affect the activities of marine mammals on 1) behavioral responses of varying severity and 2) reductions in auditory sensitivity changes, including both temporary threshold shift (TTS) and permanent threshold shift (PTS) [16], [17]. Underwater acoustic communication signals are generally mixed signals of pulse and non-pulse signals. For cetaceans, as shown in Table 1 and Table 2, the root-mean-square sound pressure levels (SPL_{rms}) thresholds of the two types of signals are different [16], [17].

TABLE 1. The effect threshold of pulse noise on cetaceans.

SPL_{rms}	Value/dB re 1μPa
Behavioral response threshold, δ	120
TTS threshold	174
PTS threshold	180

TABLE 2. The effect threshold of non-pulse noise on cetaceans.

SPL_{rms}	Value/dB re 1μPa
Behavioral response threshold, δ	160
TTS threshold	221
PTS threshold	227

In order to avoid the communication masking effect in marine mammals, the intensity of the acoustic signals transmitted to the vicinity of the marine animals should be lower than the threshold δ by adopting the detour forwarding strategy to forward the data packets. Since the proportion of the pulse or non-pulse signals in the acoustic signals is uncertain, the behavioral response threshold δ should fluctuate within the range from 120 dB re $1\mu Pa$ to 160 dB re $1\mu Pa$, according to Table 1 and Table 2.

Next, we will discuss the relationship between the source level (SL) of acoustic signals and the sound propagation distance. The transmission loss (TL) of the signal is the logarithmic function of the distance [22], i.e.,

$$TL = \kappa \cdot 10 \log d + 10^{-3} d \cdot \alpha(f), \quad (1)$$

$$\alpha(f) = \frac{0.11 f^2}{1+f^2} + \frac{44 f^2}{4100+f^2} + \frac{2.75 f^2}{10^4} + \frac{3}{10^3}, \quad (2)$$

where d represents the transmission distance in m, f represents the carrier frequency for sensor nodes in kHz, κ is the spreading factor, and $\alpha(f)$ is the absorption coefficient over frequency f in dB/km.

Hence, given the emission source level SL, the received signal level (RSL) at the transmission distance d, can be calculated by

$$RSL = SL - TL = SL - \kappa \cdot 10 \log d - 10^{-3} d \cdot \alpha(f), \quad (3)$$

According to Eq. (3) and the simulation parameters in Table 4, Fig. 4 illustrates how RSL changes with respect to transmission distance. In order to clearly illustrate the relationship between RSL and behavioral response of marine mammals, we also draw the $\mathrm{SPL_{rms}}$ threshold δ corresponding to the behavioral response of marine mammals in Fig. 4. Denote the point $(d_{\delta 0}, \delta_0)$ as the intersection point between the RSL curve and the $\mathrm{SPL_{rms}}$ threshold δ_0 curve. If the distance between a marine mammal and a sensor node is less than $d_{\delta 0}$, mammal's behavior will be disturbed when the behavioral response threshold is δ_0. Thus, $d_{\delta 0}$ is defined as acoustic protection based safe distance under threshold δ_0. The safe distance should be used to determine the detour forwarding path mentioned in Section II-A. For example, the lengths of line N_2-O and line S-O in Fig. 3(c) should be longer than $d_{\delta 0}$. Points V, H and O are close to each other. For the convenience of calculation, it is assumed that the three points are at the same position. Therefore, behavioral response to marine mammals can be avoided, as long as lengths of line N_2-V and line S-H are longer than $d_{\delta 0}$.

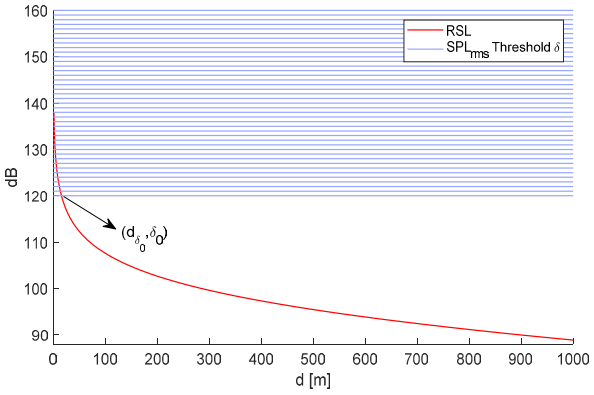

FIGURE 4. The comparison of RSL and $\mathrm{SPL_{rms}}$ threshold δ (varying with propagation distance).

Let θ represents $\angle N_2SD$ and d_1 represents the length of line S-N_2, the safe requirement can be represent as

$$\begin{cases} \sin\theta > \dfrac{d_{\delta 0}}{d_1} \\ \cos\theta > \dfrac{d_{\delta 0}}{d_1}, \end{cases} \quad (4)$$

or

$$\arcsin\left(\frac{d_{\delta 0}}{d_1}\right) < \theta < \arccos\left(\frac{d_{\delta 0}}{d_1}\right). \quad (5)$$

Thus, if θ does not meet Eq. (5), the related detour forwarding path will affect the behavior of marine mammals.

In practice, a complete data forwarding process includes multiple detour forwarding paths and non-detour forwarding paths. In the multi-hop transmission, if any wireless hop needs to take a detour, the new detour path should meet Eq. (5).

C. THE PROPOSED MF-HER PROTOCOL

In order to maximize the spectrum resource utilization, it is necessary to figure out the specific frequency range occupied by UW-ASNs and marine mammals. The frequency range of sound signals for various marine mammals is mainly concentrated at 30 Hz to 150 kHz [13]. Generally, sound signals of marine mammals can be divided into three categories: whistles, clicks, and burst pulse. With a low occurrence probability, burst pulse appears in emergency scenarios, and thus is not considered in this paper. Whistles are considered to be identification sounds to distinguish different marine mammals, while clicks are used to navigate and find preys based on echolocation [18]. The frequency range of whistles is concentrated between 30 Hz and 30 kHz, and those of clicks are higher, most of which are above 50 kHz [19]. The frequency range of UW-ASNs is mainly from 1 kHz to 40 kHz [20]. It can be seen that only whistles of the three signals have the overlapping frequency range with that of UW-ASNs.

In the proposed MF-HER protocol, sensor nodes will monitor the marine mammals' frequency range to see if any signal is detected. If yes, detour forwarding will be adopted. Note that whether or not to adopt detour forwarding depends on not only the locations of interference zones but also the marine mammals' activities. That is, if marine mammals are not using the frequency bands, non-detour forwarding path can still applied even if the path transverses the interference zones.

The packet forwarding process of the proposed MF-HER protocol is shown in Fig. 5. Once a sensor node receives a packet, the sensor node should check the following three conditions before transmitting the packet to the next sensor node, i.e., 1) Is there an interference zone between the current node and the destination node? 2) Is there any sound signals from marine mammals detected? 3) Are the detected sound signals whistles? Once the three conditions are all met, the detour forwarding path should be adopted to forward the data packets; otherwise, the non-detour forwarding path will be adopted. Note that a valid detour forwarding path should meet Eq. (5); otherwise, we have to find another valid detour forwarding path. As compared to the existing BF-CAR protocol, which chooses detour strategy as long as there is an interference zone, the proposed MF-HER in this paper reduces the waste of spectrum resources in underwater acoustic channels.

D. THE PROBABILITY OF MARINE MAMMAL IN UW-ASNS

Denote p as the probability of marine mammals being in a UW-ASN. The value of p can be estimated by the number

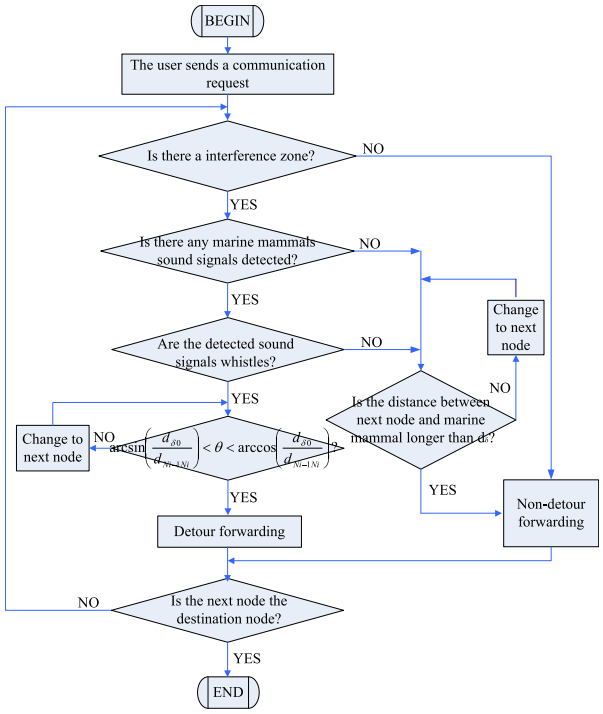

FIGURE 5. The flow chart of the proposed MF-HER protocol.

of detour forwarding paths divided by the total number of forwarding paths for a complete data transmission process, i.e.,

$$p = \frac{N_{\text{detour}}}{N_{\text{detour}} + N_{\text{non-detour}}}, \tag{6}$$

where N_{detour} and $N_{\text{non-detour}}$ are the number of detour forwarding paths and non-detour forwarding paths in a data transmission task for a UW-ASN, respectively.

Normally, living creature including marine mammals schedule their days of work and rest according to the rhythms of their biological clocks. We can get the specific time of their various life behaviors in one day by the means of ecological statistics. In addition, the sound frequency range corresponding to various behaviors can be also known by the ecological means. Thus, we can know the probability of marine mammals using an overlap frequency range with the underwater acoustic communications over a certain period of time. By utilizing the information, more detour forwarding paths can be avoided when the marine mammals, whose interference zones are overlapped with the non-detour forwarding path, do the use frequency range.

Here is an example of Sousa chinensis in Xiamen sea area to explain the above method in detail. First, the living habits of Sousa chinensis are investigated in a specific sea area. In the wild, some behaviors of Sousa chinensis have been observed, such as predatory, travelling, training, leading, and competition. Second, the schedule of each behavior and the corresponding frequency range are traced and obtained. For Sousa chinensis, predation mostly occurs in the morning and there is an associate peak at night [21], and they send clicks when predation. List the schedule in a day is shown in Table 3,

TABLE 3. The schedule of sousa chinensis in one day.

Signal Type	Behavior	Time	Probability
Clicks	Foraging	Morning	p_1
Clicks	Foraging	Evening	p_2
Whistles	Adjustment Direction	–	p_3
Clicks	Locating	–	p_4
...	...	...	...

where p_{i} (i $=$ $1, 2, 3, 4, \ldots$) is the specific probability of behavior at any given time that leads to detour forwarding.

III. PERFORMANCE EVALUATION

We will compare the performances of the proposed MF-HER protocol and that of the existing BF-CAR protocol in terms of energy consumption, bit error rate and network throughput.

A. THE ENERGY CONSUMPTION

Energy consumption is an important factor to design a network routing protocol for UW-ASNs. The main energy consumption of an underwater senor node is its underwater acoustic modem. According to the parameters of the underwater acoustic modem in [24], the energy consumption of sending packets is 40 times higher than that of receiving packets. Hence, we only consider the transmitting energy consumption in the paper. The attenuation of the power with respect to the distance d and the frequency f is denoted as $\boldsymbol{A}(d, f)$, and P_{r} is the lowest power level at which the data packet can be successfully received by the receiver. Then, the lowest transmission power of the transmitter Pt is

$$P_{\text{t}} = P_{\text{r}} \cdot A\,(d, f), \tag{7}$$

where $A(d, f)$ is the numerical form of TL in Eq. (1), and can be expressed as [27]

$$A\,(d, f) = d^{\kappa} \cdot \lambda^{10^{-3} d}, \tag{8}$$

where λ is an intermediate variable and can be expressed as

$$\lambda = 10^{\alpha(f)/10}. \tag{9}$$

The optimal operating frequency is determined by the transmission distance [22], [25], i.e.,

$$f_{\text{opt}}\,(d) = \left(\frac{200}{10^3 \cdot d}\right)^{2/3}, \tag{10}$$

where d is the transmission distance in meter, and f_{opt} is the optimal operating frequency in kHz.

By combining Eqs. (7)-(9), the energy consumption of transmitting data is

$$\begin{aligned} E &= P_{\text{t}} \cdot T_{\text{p}} \\ &= P_{\text{r}} \cdot T_{\text{p}} d^{\kappa}\, 10^{10^{-4} d \cdot \alpha(f)}, \end{aligned} \tag{11}$$

where T_{p} is the duration of transmitting data at the transmitter node, which is

$$T_{\text{p}} = \frac{l_{\text{total}}}{R_{\text{bit}}}, \tag{12}$$

where l_{total} is the size of data packet being transmitted in bit, and R_{bit} is the data rate in bit/s.

Suppose the (n, k, t) block code is applied, where n is the length of group, k is the length of load, and t is the error correction capability. The total packet length can be computed as

$$l_{\text{total}} = \frac{n}{k} l_{\text{appdata}} + l_{\text{control}}, \tag{13}$$

where l_{appdata} is the size of data packet load, and l_{control} is the size of control data packet.

As shown in Fig. 3 (c), when the forwarding path is S-N_2(/N_3)-D, the energy consumption of sending l_{total} length of data for one detour forwarding path is

$$E_{\text{detour}}(d_1) = 2P_{\text{r}} \cdot \frac{l_{\text{total}}}{R_{\text{bit}}} d_1^{\kappa} 10^{10^{-4} d_1 \alpha(f)}, \tag{14}$$

where d_1 is the distance from S to N_2 or from N_2 to D.

We assume the non-detour forwarding path is S-H-D. Then the energy consumption of one non-detour forwarding path is

$$E_{\text{non-detour}}(d_0) = 2P_{\text{r}} \cdot \frac{l_{\text{total}}}{R_{\text{bit}}} d_0^{\kappa} 10^{10^{-4} d_0 \alpha(f)}, \tag{15}$$

where d_0 is the distance from S to H or from H to D. According to the geometric relationship in Fig. 3(c), we have

$$d_0 = d_1 \cdot \cos\theta, \tag{16}$$

where θ is $\angle N_2SH$.

The energy consumption of BF-CAR is

$$E_{\text{BF-CAR}} = E_{\text{detour}}(d_1) \cdot \zeta, \tag{17}$$

where ζ is the sum of the detour forwarding times and non-detour forwarding times for one packet transmission from the source node to the destination node.

The energy consumption of MF-HER is

$$\begin{aligned} &E_{\text{MF-HER}}(\theta, p) \\ &\quad = E_{\text{detour}}(d_1) \cdot \zeta \cdot p + E_{\text{non-detour}}(d_0) \cdot \zeta \cdot (1-p) \\ &\quad = E_{\text{detour}}(d_1) \cdot \zeta \cdot p + E_{\text{non-detour}}(d_1, \theta) \cdot \zeta \cdot (1-p), \end{aligned} \tag{18}$$

where p is the proportion of detour forwarding in a total forwarding from the source node to the destination node, as calculated in Eq. (6).

To better demonstrate the performance gain of the proposed algorithm, we define the ratio of energy consumption of the two protocols as

$$R^{ECR} = \frac{E_{\text{MF-HER}}}{E_{\text{BF-CAR}}}. \tag{19}$$

B. BIT ERROR RATE

Depending on the transmission range and modulation method, the bit error rate (BER) of underwater acoustic data transmission will be different. Nowadays, frequency shift keying (FSK) and phase shift keying (PSK) are mainly adopted in underwater acoustic transmission for UW-ASNs. In this paper, we choose FSK modulation as an exapmle.

Let BER^{FSK} represents the BER in FSK modulation, which can be calculated as [26]

$$BER^{\text{FSK}} = \frac{1}{2} e^{-\frac{E_{\text{b}}/N_0}{2}}, \tag{20}$$

where E_{b}/N_0 is defined as [26]

$$E_{\text{b}}/N_0 = SNR \frac{B_{\text{N}}}{R_{\text{bit}}}, \tag{21}$$

where SNR is the signal noise ratio, and B_N is bandwidth noise. SNR is estimated based on

$$SNR = SL - TL - NL, \tag{22}$$

where NL is the noise level of receiver node in dB. Plugging Eqs. (1), (21), and (22) into Eq. (20), we have

$$\begin{aligned} BER^{\text{FSK}} &= \frac{1}{2} e^{-\frac{B_N}{2R_{\text{bit}}} \cdot SNR} \\ &= \frac{1}{2} e^{-\frac{B_N}{2R_{\text{bit}}} \cdot (SL-NL)} \cdot e^{\frac{B_N}{2R_{\text{bit}}} \cdot TL} \\ &= \frac{1}{2} e^{-\frac{B_N}{2R_{\text{bit}}} \cdot (SL-NL)} \cdot e^{\frac{B_N}{2R_{\text{bit}}} \cdot (\kappa \cdot 10 \log d + 10^{-3} d \cdot \alpha)}. \end{aligned} \tag{23}$$

The BER of one detour forwarding is

$$\begin{aligned} &BER^{\text{FSK}}_{\text{detour}}(d_1) \\ &\quad = 1 - \left(1 - BER^{\text{FSK}}\Big|_{d=d_1}\right)^2 \\ &\quad = 1 - \left(1 - \frac{1}{2} e^{-\frac{B_N}{2R_{\text{bit}}} \cdot (SL-NL)} \cdot e^{\frac{B_N}{2R_{\text{bit}}} \cdot (\kappa \cdot 10 \log d_1 + 10^{-3} d_1 \cdot \alpha)}\right)^2 \end{aligned} \tag{24}$$

The BER of one non-detour forwarding is

$$\begin{aligned} &BER^{\text{FSK}}_{\text{non-detour}}(d_0) \\ &\quad = 1 - \left(1 - BER^{\text{FSK}}\Big|_{d=d_0}\right)^2 \\ &\quad = 1 - \left(1 - \frac{1}{2} e^{-\frac{B_N}{2R_{\text{bit}}} \cdot (SL-NL)} \cdot e^{\frac{B_N}{2R_{\text{bit}}} \cdot (\kappa \cdot 10 \log d_0 + 10^{-3} d_0 \cdot \alpha)}\right)^2 \end{aligned} \tag{25}$$

The BER of BF-CAR protocol for the multi-hop UW-ASNs is

$$BER^{\text{FSK}}_{\text{BF-CAR}} = 1 - \left(1 - BER^{\text{FSK}}_{\text{detour}}\right)^{\zeta} \tag{26}$$

The BER of MF-HER protocol for the multi-hop UW-ASNs can be derived as

$$\begin{aligned} &BER^{\text{FSK}}_{\text{MF-HER}}(\theta, p) \\ &\quad = 1 - \left[1 - BER^{\text{FSK}}_{\text{detour}}(d_1)\right]^{\zeta \cdot p} \\ &\qquad \cdot \left[1 - BER^{\text{FSK}}_{\text{non-detour}}(\theta, d_1)\right]^{\zeta \cdot (1-p)} \end{aligned} \tag{27}$$

Similarly, the ratio of the BER for the two protocols is:

$$R^{BER} = \frac{BER^{\text{FSK}}_{\text{MF-HER}}}{BER^{\text{FSK}}_{\text{BF-CAR}}}. \tag{28}$$

C. NETWORK THROUGHPUT

The network throughput is the number of information bits successfully tranmitted to destination nodes per second. So it can be defined as [26]

$$NT = \frac{l_{\text{appdata}}\,(1 - PER_{\text{e2e}})}{T_{\text{flow}}}, \tag{29}$$

where T_{flow} is the end to end delay and PER_{e2e} is the end to end packet error rate, which can be computed as [26]

$$PER_{\text{e2e}} = 1 - \prod_{i=1}^{N_{\text{hop}}} \left(1 - PER_i^{\text{FEC}}\right), \tag{30}$$

where N_{hop} is the number of multi-hop, PER_i^{FEC} is the packet error rate (PER) in i-th hop when the forward error correction (FEC) coding method is applied. If the (n, k, t) block code is applied, PER_i^{FEC} is given as [26]

$$PER_i^{FEC} = 1 - (1 - ERR)^{\frac{l^{\text{appdata}}}{k}}, \tag{31}$$

where ERR is the group error rate, i.e., the probability that the number of error bits exceeds t when transmitting packets as a group. In random wireless channels, ERR can be calculated as [26]

$$ERR = \sum_{i=t+1}^{n} C_n^i BER^{\text{FSK}^i} \left(1 - BER^{\text{FSK}}\right)^{n-i}, \tag{32}$$

In a digital communications system, the probability of t errors occurring at the same time in a code group is far greater than that of $(t + 1)$ [28], so Eq. (32) can be transformed into

$$ERR \approx C_n^{(t+1)} \left(BER^{\text{FSK}}\right)^{(t+1)} \cdot \left(1 - BER^{\text{FSK}}\right)^{n-(t+1)} \tag{33}$$

Then, PER_{e2e} for BF-CAR is:

$$PER_{\text{e2e}}^{\text{BF-CAR}} = 1 - \left(1 - ERR|_{d=d_1}\right)^{2\zeta \cdot \frac{l^{\text{appdata}}}{k}}, \tag{34}$$

where $ERR|_{d=d_1}$ can be obtained from Eq. (33).

And PER_{e2e} for MF-HER is computed as

$$\begin{aligned} &PER_{\text{e2e}}^{\text{MF-HER}}(\theta, p) \\ &= 1 - \left(1 - ERR|_{d=d_1}\right)^{2\zeta p \cdot \frac{l^{\text{appdata}}}{k}} \\ &\quad \cdot \left(1 - ERR|_{d=d_0}\right)^{2\zeta(1-p) \cdot \frac{l^{\text{appdata}}}{k}} \\ &= 1 - \left(1 - ERR|_{d=d_1}\right)^{2\zeta p \cdot \frac{l^{\text{appdata}}}{k}} \\ &\quad \cdot \left(1 - ERR|_{d=d_1 \cos\theta}\right)^{2\zeta(1-p) \cdot \frac{l^{\text{appdata}}}{k}}, \end{aligned} \tag{35}$$

where $ERR|_{d=d_0}$ can be obtained from Eq. (33).

In general, the end to end delay T_{flow} in Eq. (29) consists of four items: processing delay, queuing delay, transmission delay and propagation delay. In UW-ASNs, the processing delay is negligible. When the network load is low, the queuing delay is also much lower than the transmission delay and propagation delay. Therefore, T_{flow} can be written as [26]

$$T_{\text{flow}} = T_{\text{propagation}} + T_{\text{transmission}}, \tag{36}$$

where $T_{\text{propagation}}$ is propagation delay, and $T_{\text{transmission}}$ is the transmission delay. Let v be the propagation speed of underwater acoustic. Then, the propagation delay of one non-detour forwarding and one detour forwarding are

$$T_{\text{propagation}}^{\text{non-detour}} = 2 \cdot \frac{d_0}{v}, \tag{37}$$

$$T_{\text{propagation}}^{\text{detour}} = 2 \cdot \frac{d_1}{v}. \tag{38}$$

Hence, the propagation delay of BF-CAR and MF-HER are

$$T_{\text{propagation}}^{\text{BF-CAR}} = \zeta \cdot T_{\text{propagation}}^{\text{detour}} = 2\zeta \cdot \frac{d_1}{v}, \tag{39}$$

$$\begin{aligned} T_{\text{propagation}}^{\text{MF-HER}} &= \zeta p \cdot T_{\text{propagation}}^{\text{detour}} + \zeta(1-p) \cdot T_{\text{propagation}}^{\text{non-detour}} \\ &= 2\zeta p \cdot \frac{d_1}{v} + 2\zeta(1-p) \cdot \frac{d_0}{v} \\ &= 2\zeta p \cdot \frac{d_1}{v} + 2\zeta(1-p) \cdot \frac{d_1 \cos\theta}{v}, \end{aligned} \tag{40}$$

In addition, $T_{\text{transmission}}$ includes receiving delay and forwarding delay [26], i.e.,

$$\begin{aligned} T_{\text{transmission}} &= T_{\text{recv}} + T_{\text{forwd}} \\ &= 2 \cdot 2\zeta \cdot \left(\frac{l_{\text{total}}}{R_{\text{bit}}} + T_{\text{dec}}\right) \\ &\approx 4\zeta \cdot \frac{l_{\text{total}}}{R_{\text{bit}}}, \end{aligned} \tag{41}$$

where T_{recv} is receiving delay, T_{forwd} is forwarding delay, T_{dec} is the decoding delay, and l_{total} is the size of the data packets when FEC transmission mechanism is adopted. Here, $T_{dec}$is neglected and l_{total} is derived based on Eq. (13).

Thus, the end-to-end delay of BF-CAR is

$$T_{\text{flow}}^{\text{BF-CAR}}(d_1) = 2\zeta \cdot \frac{d_1}{v} + 4\zeta \cdot \frac{(n \cdot l_{\text{appdata}} + k \cdot l_{\text{control}})/k}{R_{\text{bit}}} \tag{42}$$

The end to end delay of MF-HER is

$$\begin{aligned} T_{\text{flow}}^{\text{MF-HER}}(\theta, p) &= 2\zeta p \cdot \frac{d_1}{v} + 2\zeta(1-p) \cdot \frac{d_1 \cos\theta}{v} \\ &\quad + 4\zeta \cdot \frac{(n \cdot l_{\text{appdata}} + k \cdot l_{\text{control}})/k}{R_{\text{bit}}} \end{aligned} \tag{43}$$

Finally, the throughput of BF-CAR can be derived as

$$NT^{\text{BF-CAR}} = \frac{l_{\text{appdata}}\left(1 - PER_{\text{e2e}}^{\text{BF-CAR}}\right)}{T_{\text{flow}}^{\text{BF-CAR}}}. \tag{44}$$

The throughput of MF-HER protocol can be derived as

$$NT^{\text{MF-HER}}(\theta, p) = \frac{l_{\text{appdata}}\left[1 - PER_{\text{e2e}}^{\text{MF-HER}}(\theta, p)\right]}{T_{\text{flow}}^{\text{MF-HER}}(\theta, p)}. \tag{45}$$

Then the ratio of network throughout for the two protocols is

$$R^{NT} = \frac{NT^{\text{MF-HER}}}{NT^{\text{BF-CAR}}}. \tag{46}$$

IV. SIMULATION EVALUATION

From Eqs. (18), (27) and (45), we know that the values for energy consumption, bit error rate, and network throughput depend on p and θ. In the simulation, we will evaluate how the two parameters impact on the energy consumption, bit error rate, and throughput of the proposed MF-HER protocol and existing BF-CAR protocol will be studied. The simulation parameters are listed in Table 4.

TABLE 4. Simulation parameters.

Parameter	Value	Parameter	Value
κ	1.5	ζ	30
R_{bit}	10 kbit/s	l_{control}	10 bit
B_{N}	20 kHz	l_{appdata}	300 bit
d_1	1000 m	n	128
d_0	$(d_1 \cdot \cos\theta)$ m	k	78
v	1500 m/s	t	3
SL	138 dB	NL	81.24 dB
f	20 kHz		

If θ can satisfy Eq. (5), underwater acoustic communications will not hinder the behavior of marine mammals. The value of acoustic protection based safe distance $d_{\delta 0}$ changes constantly with the SPL_{rms} threshold δ, as shown in Fig. 6, which is determined by Eq. (3) and Fig. 4.

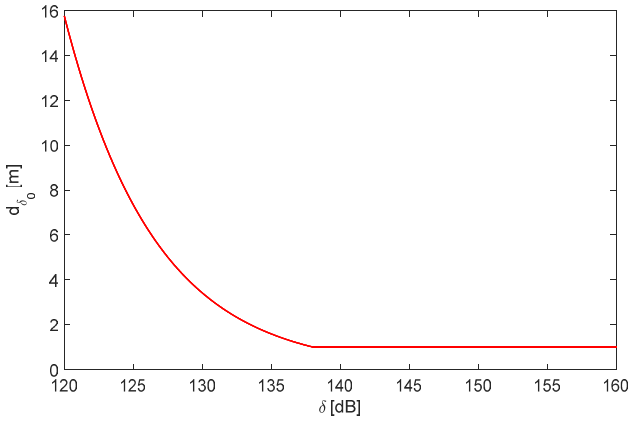

FIGURE 6. The curve of acoustic protection based safe distance $d_{\delta 0}$ changes with δ.

It can be seen from Fig. 6 that with the increasing of δ, the acoustic protection based safe distance $d_{\delta 0}$ is reduced. When δ equals to 138 dB, $d_{\delta 0}$ is about 1 m. If δ continues increasing, the value of $d_{\delta 0}$ is also set at 1 m to protect the sensor node. Also, no matter what value δ is selected, the behavior of marine mammals is not affected as long as $d_{\delta 0}$ is no less than to 16 m. Therefore, we let $d_{\delta 0}$ equal to 16 m.

As shown in Fig. 1, the sensor nodes are deployed in a three-dimensional space. The distance between sensor nodes and marine mammals considered in this paper is the distance projected on the seabed from the actual distance in three-dimensional space. Therefore, the real distance in three-dimensional space should be longer than the calculated distance herein, thus guaranteeing that there will be no behavioral hindrance to marine mammals.

A. ENERGY CONSUMPTION

As we can see from Figs. 7(a) and 7(c), given the value of p, the energy consumption of MF-HER decreases gradually, and the ratio of energy consumption of MF-HER and BF-CAR also decreases as θ increases. A larger θ incurs a larger ratio of the energy consumption of a detour forwarding path and the energy consumption of a non-detour forwarding path. If θ equals to 0°, the energy consumption of the two forwarding paths are exactly the same, and so the energy consumption of the two protocols are the same. When θ infinity approaches to 90°, the distance of the detour forwarding approaches to infinity, and the distance of the non-detour forwarding becomes a small value. Then, the ratio is infinitely close to p.

In Fig. 7(b) and 7(d), the ratio of energy consumption of MF-HER and that of BF-CAR increases as p increases. When p increases, the number of the detour forwarding paths in MF-HER increases and the energy consumption ratio of the two protocols also increases. When p is equal to 0, all of the forwarding paths in MF-HER is non-detour.

The proposed MF-HER protocol incurs lower energy consumption as compared to BF-CAR under different values of θ and p. This is because, in general, detour forwarding path consumes more energy than non-detour forwarding path, and the proposed MF-HER protocol avoids unnecessary detours and thus consumes less energy.

B. BIT ERROR RATE

From Figs. 8(a) and 8(c), it can be observed that the BER of the protocol MF-HER decreases as θ increases. When θ is equal to 0, the two forwarding schemes are the same, and so the BER of the two protocols are also equal. Suppose that d_1 is a constant, and then, d_0 reduces as θ increases. The BER of the non-detour forwarding path is smaller than that of detour forwarding path. In that case, the advantage of the proposed MF-HER protocol, which avoids many detour forwarding paths in BF-CAR, is obvious. Therefore, the BER of the proposed MF-HER protocol is lower than that of BF-CAR.

From Figs. 8(c) and 8(d), we can see that with the increase of p, the BER of MF-HER increases, and gradually approaches to that of BF-CAR. When p equals to 1, the selected forwarding paths of the two protocols are the same. While the value of p is between 0 and 0.6, the advantages of the proposed MF-HER protocol are more obvious, i.e., the BER can be greatly reduced by considering the probability of marine mammals for the proposed MF-HER protocol.

C. NETWORK THROUGHPUT

Fig. 9(a) shows that when θ increases, the network throughput increases. When θ rises, the distance of the non-detour forwarding path reduces and the difference between the two protocols in PER or end to end delay increases, and thus

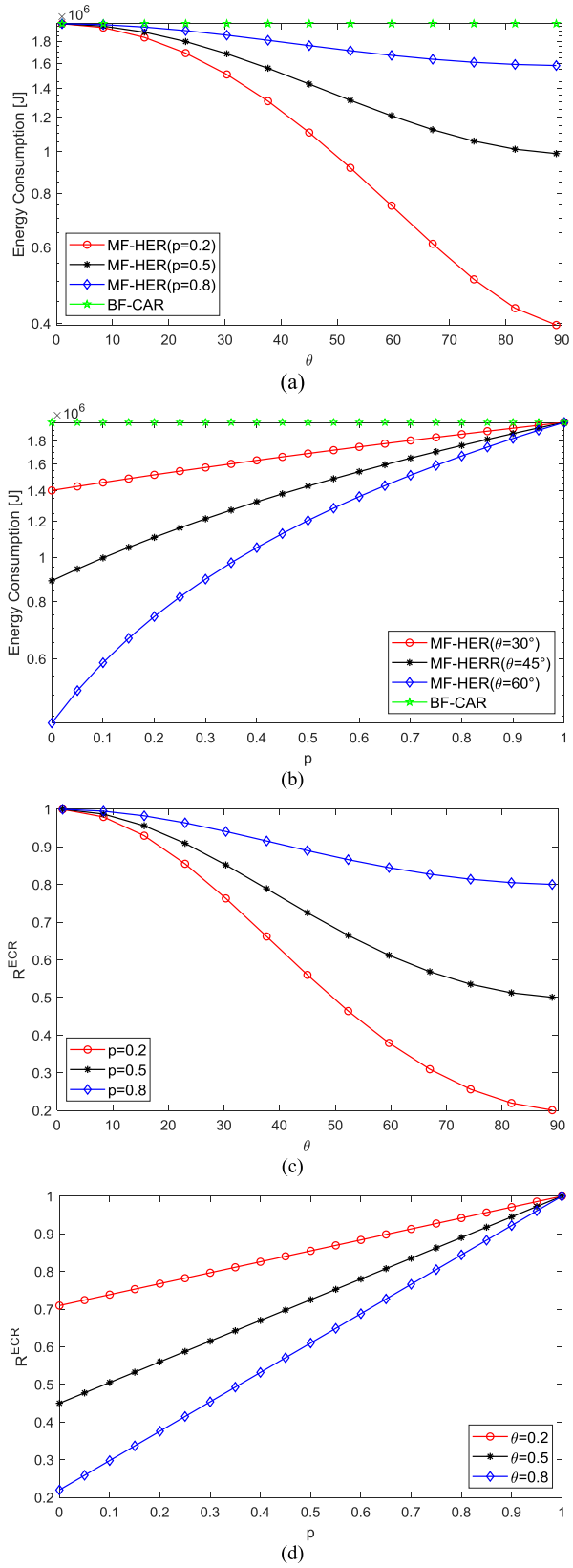

FIGURE 7. The energy consumption of the two protocols: (a) the curve of the energy consumption with θ; (b) the curve of the energy consumption with p; (c) the curve of the energy consumption ratio with θ; (d) the curve of the energy consumption ratio with p.

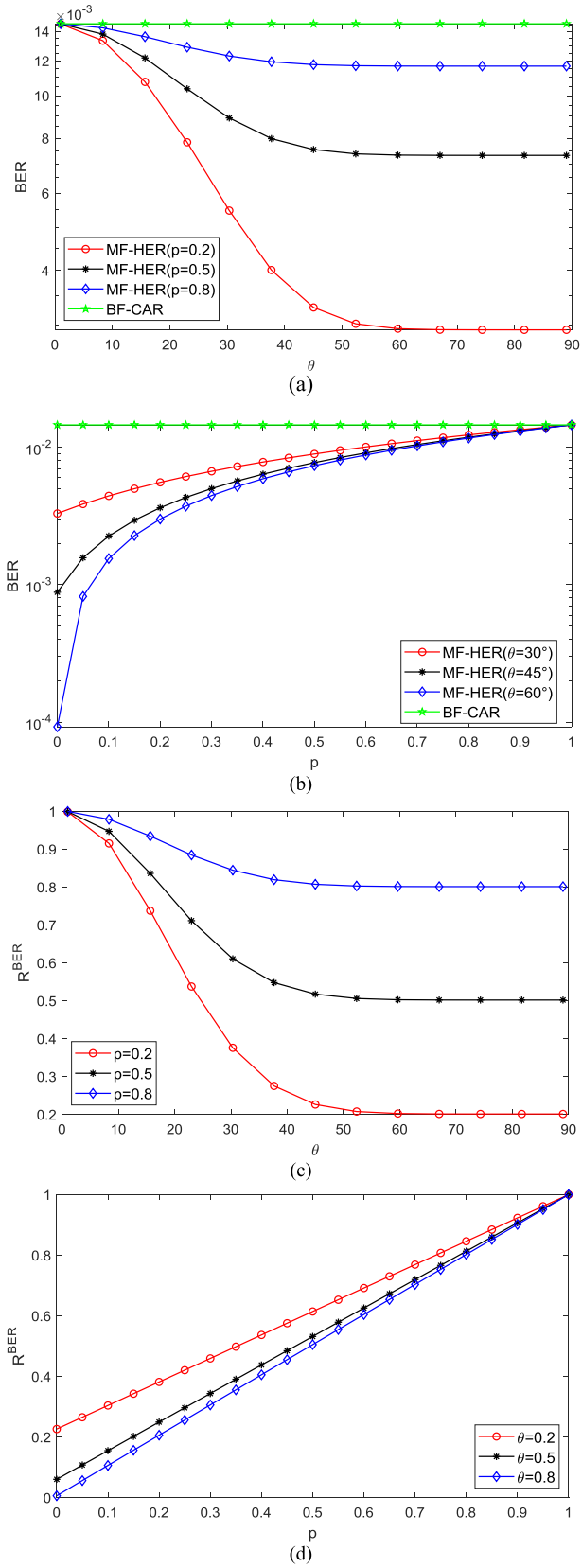

FIGURE 8. The BER of the two protocols: (a) the curve of BER with θ; (b)the curve of BER with p; (c) the curve of BER with θ; (d) the curve of BER with p.

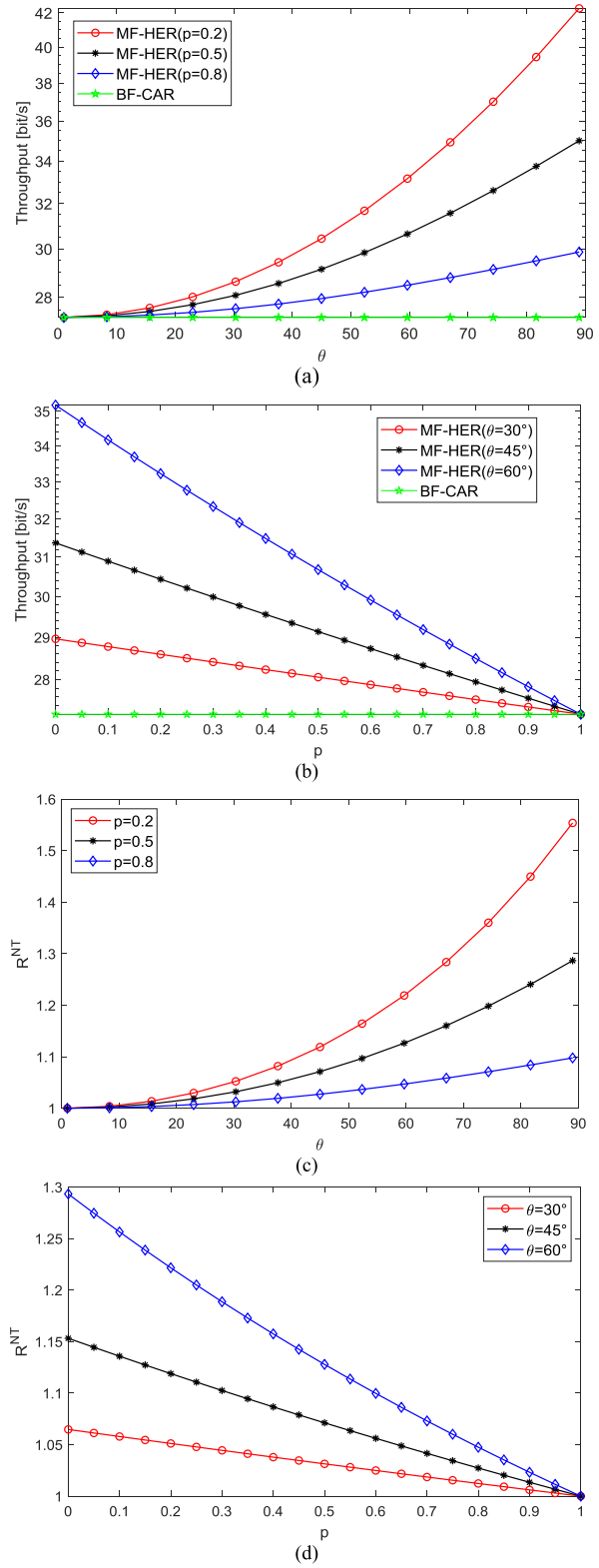

FIGURE 9. The network throughput of the two protocols: (a) the curve of the network throughput with θ; (b) the curve of the network throughput with p; (c) the curve of the network throughput ratio with θ; (d) the curve of the network throughput ratio with p.

the gap between the protocols in network throughput also becomes larger. From Figs. 9(a) and 9(b), it can be seen that θ has a greater impact on network throughput than p. Therefore, if we want to improve the performance of network throughput, it is recommended to increase the value of θ appropriately.

It can be seen from Fig. 9(c) that the network throughput decreases gradually as p increases. A larger p reduces the BER as well as the PER. At the same time, the delay will also increase. However, the change of PER is smaller than that of end to end delay. As the p increases, the network throughput decreases, which is demonstrated in Fig. 9(d).

Therefore, the proposed MF-HER protocol can significantly improve network throughput as compared to the existing BF-CAR protocol by avoiding unnecessary detours and making necessary detour forwarding in response to marine mammal behaviors.

V. CONCLUSION

Based on the BF-CAR protocol, this paper proposes a novel routing scheme, i.e., MF-HER, for UW-ASNs by considering the acoustic protection for marine mammals. Considering the overlap of the frequency range of marine mammals' vocal signals and the occupied frequency range of UW-ASNs, the detour forwarding is adopted to avoid the interference from sensor nodes to marine mammals while shortening the multi-hop path distance. The energy consumption, BER, and network throughput of the proposed MF-HER protocol are deduced. The simulation results show that the proposed MF-HER protocol outperforms the BF-CAR protocol.

ACKNOWLEDGMENT

The authors would like to thank Dr. Xiaokang Zhang, Mr. Shenqin Huang, and Mr. Jianming Wu from Xiamen University for their contributions to the discussion of this research. Part of this work has been presented [30] at 2019 IEEE International Conference on Signal Processing, Communications and Computing, ICSPCC2019, Dalian, China, Sep. 20-23, 2019. Shenzhen Research Institute of Xiamen University and Key Laboratory of Underwater Acoustic Communication and Marine Information Technology (Xiamen University), Ministry of Education, contributed equally to this work.

REFERENCES

[1] Q. Guan, F. Ji, Y. Liu, H. Yu, and W. Chen, "Distance-vector-based opportunistic routing for underwater acoustic sensor networks," *IEEE Internet Things J.*, vol. 6, no. 2, pp. 3831–3839, Apr. 2019.

[2] K. M. Pouryazdanpanah, M. Anjomshoa, S. A. Salehi, A. Afroozeh, and G. M. Moshfegh, "DS-VBF: Dual sink vector-based routing protocol for underwater wireless sensor network," in *Proc. IEEE 5th Control Syst. Graduate Res. Colloq.*, Aug. 2014, pp. 227–232.

[3] T. Hu and Y. Fei, "QELAR: A machine-learning-based adaptive routing protocol for energy-efficient and lifetime-extended underwater sensor networks," *IEEE Trans. Mobile Comput.*, vol. 9, no. 6, pp. 796–809, Jun. 2010.

[4] J. Jiang and G. Han, "Routing protocols for unmanned aerial vehicles," *IEEE Commun. Mag.*, vol. 56, no. 1, pp. 58–63, Jan. 2018.

[5] P. Jiang, X. Wang, and L. Jiang, "Node deployment algorithm based on connected tree for underwater sensor networks," *Sensors*, vol. 15, no. 7, pp. 16763–16785, Jul. 2015.

[6] S. Coatelan and A. Glavieux, "Design and test of a multicarrier transmission system on the shallow water acoustic channel," in *Proc. OCEANS*, Brest, France, 1994, pp. 472–477.

[7] A. A. Syed and J. Heidemann, "Time synchronization for high latency acoustic networks," in *Proc. IEEE 25TH IEEE Int. Conf. Comput. Commun. (INFOCOM)*, Barcelona, Spain, Apr. 2006, pp. 1–12.

[8] P. Xie, J.-H. Cui, and L. Lao, "VBF: Vector-based forwarding protocol for underwater sensor networks," in *Proc. Netw.*, 2006, pp. 1216–1221.

[9] N. Nicolaou, A. See, P. Xie, J.-H. Cui, and D. Maggiorini, "Improving the robustness of location-based routing for underwater sensor networks," in *Proc. OCEANS Eur.*, Jun. 2007, pp. 1–6.

[10] C. Su, X. Liu, and F. Shang, "Vector-based low-delay forwarding protocol for underwater wireless sensor networks," in *Proc. Int. Conf. Multimedia Inf. Netw. Secur.*, 2010, pp. 178–181.

[11] X. Xiao, X. P. Ji, G. Yang, and Y. P. Cong, "LE-VBF: Lifetime-extended vector-based forwarding routing," in *Proc. Int. Conf. Comput. Sci. Service Syst.*, Aug. 2012, pp. 1201–1203.

[12] G. Yao, Z. Jin, and Y. Su, "An environment-friendly spectrum decision strategy for underwater wireless sensor networks," in *Proc. IEEE Int. Conf. Commun. (ICC)*, London, U.K., Jun. 2015, pp. 6370–6375.

[13] Z. Jin, J. Wang, and Y. Su, "A routing protocol of underwater cognitive acoustic networks for marine mammals," *J. Xi'an Jiaotong Univ.*, vol. 51, no. 2, pp. 33–39, Feb. 2017.

[14] S. Liu, B. Liu, Y. Yin, and G. Qiao, "M-ray covert underwater acoustic communication by mimicking dolphin sounds," *J. Harbin Eng. Univ.*, vol. 35, no. 1, pp. 119–125, Jan. 2014.

[15] G. Su, "Study on the impact of underwater pile-driving noise on rare marine mammals (Chinese white dolphin and spotted seal) in China Sea," M.S. thesis, Dept. Appl. Mar. Phys. Eng., Xiamen Univ., Xiamen, China, 2013.

[16] R. Oestman, D. Buehler, J. Reyff, and R. Rodkin, "Technical guidance for assessment and mitigation of the hydroacoustic effects of pile driving on fish," ICF Int., Rep. California Dept. Transp. (Caltrans), Sacramento, CA, USA, Tech. Rep., 2009. [Online]. Available: https://tethys.pnnl.gov/publications/technical-guidance-assessment-mitigation-hydroacoustic-effects-pile-driving-fish

[17] B. L. Southall, J. J. Finneran, C. Reichmuth, P. E. Nachtigall, D. R. Ketten, A. E. Bowles, W. T. Ellison, D. P. Nowacek, and P. L. Tyack, "Marine mammal noise exposure criteria: Updated scientific recommendations for residual hearing effects," *Aquatic Mammals*, vol. 45, no. 2, pp. 125–232, Mar. 2019.

[18] L. Yang, X. Tu, Q. Wang, Z. Zhu, and X. Xu, "Autocorrelation method for time delay estimation to calculate the source level of click signal for Sousa Chinensis," in *Proc. OCEANS TAIPEI*, Taipei, Taiwan, Apr. 2014, pp. 1–5.

[19] Z. Jin, J. Wang, and Y. Su, "Marine Mammal-friendly Spectrum Allocation Algorithm for Cognitive Underwater Acoustic network," *J. Jilin Univ., Eng. Technol. Ed.*, vol. 47, no. 4, pp. 1321–1328, Jul. 2017.

[20] Y. Luo, L. Pu, M. Zuba, Z. Peng, and J.-H. Cui, "Cognitive acoustics: Making underwater communications environment-friendly," in *Proc. Int. Conf. Underwater Netw. Syst. (WUWNET)*, no. 48, Jan. 2014, pp. 1–2.

[21] L. Zhang, X. Xu, and C. Wei, "Comparison between indo-pacific bottlenose dolphin (Tursiops aduncus) and indo-pacific humpback dolphin (Sousa Chinensis) whistle," *Tech. Acoust.*, vol. 30, no. 5, pp. 41–44, Oct. 2011.

[22] M. Stojanovic, "On the relationship between capacity and distance in an underwater acoustic communication channel," *ACM SIGMOBILE Mobile Comput. Commun. Rev.*, vol. 11, no. 4, pp. 41–47, Nov. 2006.

[23] C. Li, Y. Xu, B. Diao, Q. Wang, and Z. An, "DBR-MAC: A depth-based routing aware MAC protocol for data collection in underwater acoustic sensor networks," *IEEE Sensors J.*, vol. 16, no. 10, pp. 3904–3913, May 2016.

[24] S. Sendra, J. Lloret, J. M. Jimenez, and L. Parra, "Underwater acoustic modems," *IEEE Sensors J.*, vol. 16, no. 11, pp. 4063–4071, Jun. 2015.

[25] Y. Wei and D.-S. Kim, "Reliable and energy-efficient routing protocol for underwater acoustic sensor networks," in *Proc. Int. Conf. Inf. Commun. Technol. Converg. (ICTC)*, Nanjing, China, Oct. 2014, pp. 185–190.

[26] X. Du and Y. Su, *Research on Underwater Sensor Network*. Beijing, China: Science Press, 2016.

[27] B. Liu and J. Lei, *Principles of Hydroacoustics*. Beijing, China: Science Press, 2019.

[28] Y. Yu, "Research on the algorithm of blind recognition about block code," M.S. thesis, Dept. Commun. Eng., Hangzhou Univ. Electron. Sci. Technol., Hangzhou, China, Jan. 2013.

[29] H. Yan and Z. J. Shir, "DBR: Depth-based routing for underwater sensor networks," in *Proc. Int. Conf. Res. Netw.* Berlin, Germany: Springer, 2008.

[30] X. Zhang, Y. Chen, J. Zhu, W. Yu, X. Zhang, and X. Xu, "A high spectral efficiency marine mammal-friendly routing protocol for underwater acoustic networks," in *Proc. IEEE Int. Conf. Signal Process., Commun. Comput. (ICSPCC)*, Dalian, China, Sep. 2019, pp. 1–5.

[31] C. Erbe, C. Reichmuth, K. Cunningham, K. Lucke, and R. Dooling, "Communication masking in marine mammals: A review and research strategy," *Mar. Pollut. Bull.*, vol. 103, nos. 1–2, pp. 15–38, Feb. 2016.

[32] J. Lossent, M. Lejart, T. Folegot, D. Clorennec, L. Di Iorio, and C. Gervaise, "Underwater operational noise level emitted by a tidal current turbine and its potential impact on marine fauna," *Mar. Pollut. Bull.*, vol. 131, pp. 323–334, Jun. 2018.

YOUGAN CHEN (Senior Member, IEEE) received the B.S. degree from Northwestern Polytechnical University (NPU), Xi'an, China, in 2007, and the Ph.D. degree from Xiamen University (XMU), Xiamen, China, in 2012, all in communication engineering.

He visited the Department of Electrical and Computer Engineering, University of Connecticut (UCONN), Storrs, CT, USA, from November 2010 to November 2012. Since 2013, he has been with the College of Ocean and Earth Sciences, XMU, where he is currently an Associate Professor of applied marine physics and engineering. His research includes the application of electrical and electronics engineering to the oceanic environment, with recent focus on cooperative communication and artificial intelligence for underwater acoustic channels. He has authored or coauthored more than 50 peer-reviewed journal/conference papers and holds more than ten China patents.

Dr. Chen has been severed as an Associate Editor of IEEE Access, since 2019. He has served as the Technical Reviewer for many journals and conferences, such as the IEEE Journal of Oceanic Engineering, IEEE Transactions on Communications, IEEE Access, *Sensors, IET Communications*, and ACM WUWNet Conference. He served as a Secretary for IEEE ICSPCC 2017 and the TPC member for IEEE ICSPCC 2019. He received Technological Invention Award of Fujian Province, China, in 2017.

XINRUI ZHANG received the B.S. degree in marine physics from Xiamen University (XMU), Xiamen, China, in 2020. She is currently pursuing the M.S. degree in signal and information processing with Southeast University (SEU), Nanjing, China. Her research interests focus on signal processing, underwater acoustic communication, and networking.

XIANG SUN (Member, IEEE) received the B.E. and M.E. degrees from the Hebei University of Engineering, in 2008 and 2011, respectively, and the Ph.D. degree in electrical engineering from the New Jersey Institute of Technology (NJIT), in 2018. He is currently an Assistant Professor of electrical and computer engineering with the University of New Mexico. His research interests include mobile edge computing, cloud computing, the Internet of Things, wireless networks, big-data-driven networking, and green communications and computing. He has also served as a TPC member of many conferences. He has received several honors and awards, including the 2016 IEEE International Conference on Communications Best Paper Award, the 2017 IEEE Communications Letters Exemplary Reviewers Award, the 2018 NJIT Hashimoto Price, the 2018 Inter Digital Innovation Award on IoT Semantic Mashup, the 2019 NJIT Outstanding Doctoral Dissertation Award, and the 2019 IEICE Communications Society Best Tutorial Paper Award. He is currently an Associate Editor *of Digital Communications and Networks*.

YI TAO (Member, IEEE) received the B.S. degree in computer science and applications from Hangzhou Dianzi University, China, in 1998, the M.S. degree in computational fluid mechanics (SIAMM) from Shanghai University, China, in 2003, and the Ph.D. degree in marine sciences from Xiamen University (XMU), China, in 2008.

Since 2008, he has been an Assistant Professor with the Department of Applied Marine Physics and Engineering, XMU. His research interests include marine acoustic signal processing and underwater acoustic communication.

XIAOMEI XU received the B.S., M.S., and Ph.D. degrees in marine physics from Xiamen University (XMU), Xiamen, China, in 1982, 1988, and 2002, respectively.

She was a Visiting Scholar with the Department of Electrical and Computer Engineering, Oregon State University, Corvallis, OR, USA, from 1994 to 1995. She visited the Department of Electrical and Computer Engineering, University of Connecticut (UCONN), Storrs, CT, USA, as a Senior Visiting Scholar, in 2012. She is currently a Full Professor with the Department of Applied Marine Physics and Engineering, XMU. Her research interests include the fields of marine acoustics, underwater acoustic telemetry and remote control, underwater acoustic communication, and signal processing.